Plasmonics (2014) 9:835–844
DOI 10.1007/s11468-014-9678-3

Development of Localized Surface Plasmon Resonance-Based Point-of-Care System

Xiaodong Zhou · Ten It Wong · Hong Yan Song · Lin Wu · Yi Wang · Ping Bai · Dong-Hwan Kim · Sum Huan Ng · Man Siu Tse · Wolfgang Knoll

Received: 31 December 2013 / Accepted: 22 January 2014 / Published online: 14 February 2014

Abstract This paper describes our point-of-care system development based on localized surface plasmon resonance (LSPR). Although LSPR has been a hot research area for a few decades, there are several bottlenecks which hampered its application for point-of-care (POC) medical diagnostics. The first is the detection sensitivity shortage when the direct LSPR wavelength shift is used for sensing, the second is the mass fabrication of durable metal nanostructures on the substrate, and the third is the microfluidic chip and the POC system which have to be combined with LSPR chips in a seamless but cost-effective way. To solve the above challenges, several novel technologies are initiated and successfully implemented in this work. To increase the sensitivity of the LSPR detection, we use plasmonic field to excite the fluorescence dyes conjugated to the analyte rather than directly detecting the LSPR wavelength shift upon analyte bonding. This method can enhance the biomarker detection sensitivity 10 to 100 times upon careful design of the metal nanostructures and the location of the fluorescence dyes in the bioassay. To mass fabricate the metal nanostructures, a 4″ nickel mold is fabricated by electroplating and employed for UV nanoimprinting lithography. Our technology achieves high yield on wafer-level mass fabrication of the designed metal nanostructures. In terms of the surface modification of the bioassay, the orientation of the capturing antibody is controlled to enhance the sensitivity of biomarker detections, and an antifouling polymer is synthesized inside the gold nanoholes. To accomplish the cost-effective point-of-care system, a plastic multichamber microfluidic chip is fabricated, which contains the metal nanostructures, microfluidic channels, and trenches for controlling the sample flow. The microfluidic chip is inserted into a point-of-care system which consists of micropumps to control the microfluidic flow, a light source for fluorescence excitation, a camera system for fluorescence detection, and software to automate the POC system and to analyze the results. We believe this highly sensitive LSPR point-of-care system has ample applications on medical diagnostics.

Keywords Localized surface plasmon resonance (LSPR) · Plasmonics · Nanofabrication · Nanoimprinting · Microfluidics · Point-of-care (POC)

X. Zhou (✉) · T. I. Wong · H. Y. Song · W. Knoll
Institute of Materials Research and Engineering, Agency for Science, Technology and Research (A*STAR), 3 Research Link, Singapore 117602, Singapore
e-mail: donna-zhou@imre.a-star.edu.sg

L. Wu · P. Bai
Electronics and Photonics Department, Institute of High Performance Computing, Agency for Science, Technology and Research (A*STAR), 1 Fusionopolis Way, Singapore 1386323, Singapore

Y. Wang · W. Knoll
Centre for Biomimetic Sensor Science, Nanyang Technological University, 50 Nanyang Drive, Research Techno Plaza 6th Storey, XFrontiers Block, Singapore 637553, Singapore

D.-H. Kim
Division of Bioengineering, School of Chemical and Biomedical Engineering, Nanyang Technological University, 637457 Singapore, Singapore

S. H. Ng
Singapore Institute of Manufacturing Technology, Agency for Science, Technology and Research (A*STAR), 71 Nanyang Drive, Singapore 638075, Singapore

M. S. Tse
School of Electrical and Electronic Engineering, Nanyang Technological University, 50 Nanyang Avenue, Singapore 639798, Singapore

W. Knoll
Austrian Institute of Technology (AIT), Donau-City-Straße 1, 1220 Vienna, Austria

Introduction

Surface plasmon resonance (SPR) is the collective oscillation of electrons on a gold film, and it is utilized for real-time

detection of biological or chemical analyte through the resonance peak shift upon the reflective index change caused by the binding of the chemicals on the gold film [1–3]. SPR has been proven to be a powerful technology for biosensing for 30 years, and the fast engineering development of the SPR instrument as well as its bioassays have facilitated and established its wide applications. However, SPR has the disadvantage of being bulky and complicated in detection (prism, grating, or waveguide is required to match the momentum of the light with the gold film), temperature sensitive (temperature stability apparatus is set in the SPR equipment), polarization sensitive, and low sensitivity (which hampers the application of SPR for medical diagnostics where high sensitivity is required). An easy substitution of SPR is the localized surface plasmon resonance (LSPR), where the electron oscillation is confined in noble metallic nanoparticles. LSPR generates easily by shedding light on the metal nanostructures, and it is neither sensitive to the light incident direction nor the temperature of the ambient, but at a cost of fabricating the gold nanostructures on the glass substrate as well as a lower sensitivity to the reflective index change [4–8].

A very useful strategy to enhance the sensitivity is to use surface plasmon enhanced fluorescence spectroscopy (SPFS) which utilizes SPR to excite the fluorescence labels of the analyte, and it has been reported that SPFS using a photomultipler (PMT) detector can detect the prostate-specific antigen (PSA), a typical biomarker in blood indicating the prostate cancer for males, as low as 2 pg/ml [9–11], which far exceeds the cutoff level of the prostate cancer screening. In contrast, the conventional SPR can only detect PSA at 300 ng/ml and without labels or 0.15 ng/ml with gold nanoparticle labels [12]. However, SPFS is bulkier than SPR equipment thus is not used for medical diagnostics but for research.

The global biosensors market is expected to grow at a compounded annual growth rate of 9.6 % from 2012 to 2018 to reach a market of USD 18.9 billion by 2018, and the applications of biosensors in medical examinations and diagnoses, typically the point-of-care (POC) systems, remain the largest market for biosensors and probably dominate the future (http://www.prweb.com/releases/2013/7/prweb10923056.htm). In our research, we combine the highly sensitive SPFS and compact LSPR chip for the development of a POC system for medical diagnostics [13–17]. As presented in Fig. 1, LSPR is used to excite the fluorescence labels for biomarker detection with a sandwich assay of "capturing antibody-antigen-detection antibody". It is well known that the sensitivity requirements for medical diagnostics are very strict; this method is much more sensitive than direct LSPR spectral test because of the dye labeling and also much more sensitive than ELISA because the fluorescence dyes are enhanced ten to hundreds of times by LSPR

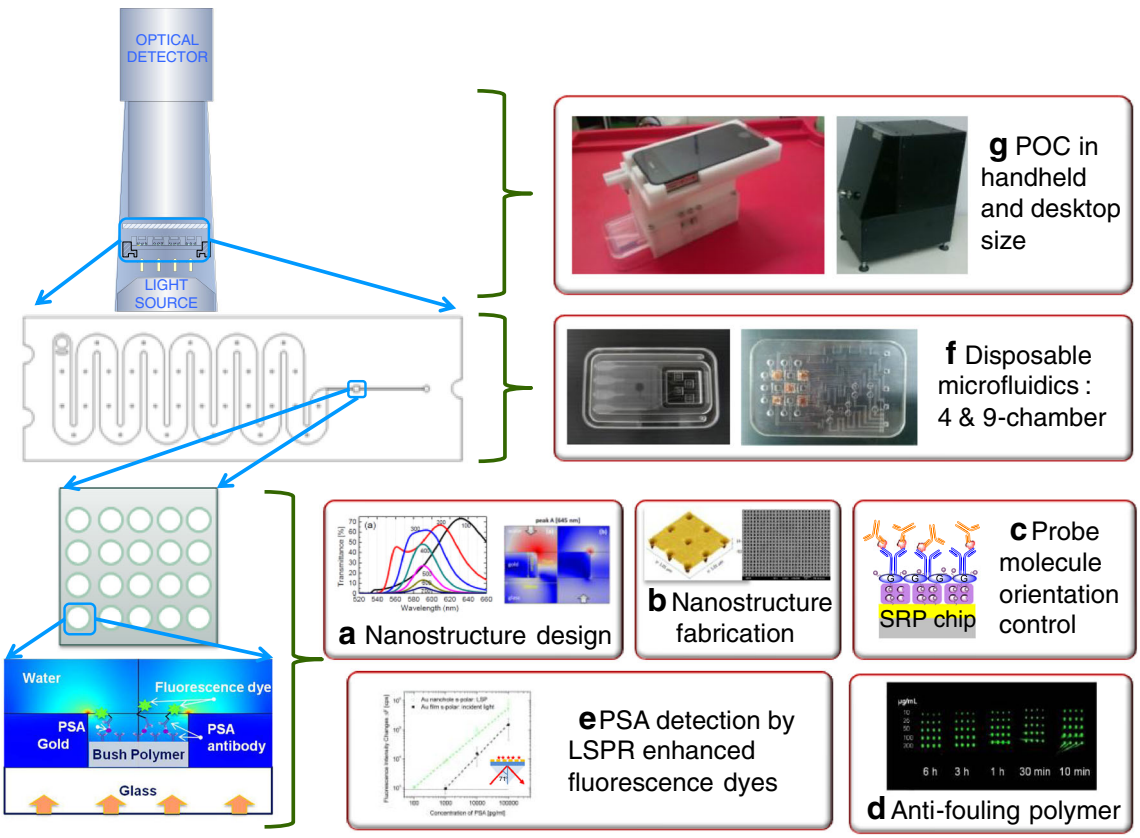

Fig. 1 The principle (*left*) and technologies developed (*right*) for forming the LSPR POC system

[18, 19]. The optical detection of our method is highly compact with just a light source and a photodetector, and this simplicity provides a perfect condition for constructing a POC system with inexpensive components and many functional integrations. The research of using LSPR for analyte detections has been published by several groups, but we are the first to use gold nanohole array for SPFS-based detection of biomarkers and the development of the POC system, and we believe our developmental details here shed light on using SPR or LSPR for POC biosensors.

Principle

Figure 1 presents the principle (left) and the technologies we have developed (right) for the LSPR-based POC system for medical diagnostics. On the left part, from the bottom to the top, first the gold nanohole array on glass substrate is designed and fabricated to excite the fluorescence labels of the analyte, the LSPR chip is then integrated with the microfluidics, and the microfluidic chip will be inserted into the POC detection system for fluorescence excitation with a light source and reading with an optical detector.

The right side of Fig. 1 demonstrates the technologies we developed to realize the principle of the POC system. Because the light source and the detector in a POC system are usually compact in size and less sensitive, the key to the success of the POC system is to achieve high sensitivity, thus several methods are adopted in our research for this purpose. Figure 1a is the design of the gold nanohole array that is able to excite plasmonics on the gold–water interface at the same wavelength of the fluorescence dyes. As the plasmonic wavelength is close to the dye excitation wavelength, the dye excitation enhancement is maximized. Figure 1b is to fabricate the gold nanohole array on glass substrate with high quality to materialize the design, and mass and cost-effective fabrication is desired. In our project, nanoimprinting is used to replace the expensive and slow e-beam lithography. Figure 1c is the orientation controlled capturing antibody (cAb) immobilization method to achieve high density cAb layer on the gold surface and the high exposure rate of the active cAb binding sites to the analyte under detection. Figure 1d is a layer of antifouling polymer poly(olygo (ethylene glycol) methacrylate) (POEGMA) to selectively bind the cAb on the desired areas while block the false binding of cAb on other places. Figure 1e is a bioassay established on gold nanostructures without using the methods in 1c and 1d to evaluate the effectiveness of our fabricated LSPR chip in increasing the sensitivity for PSA detection. Figure 1f presents the microfluidic chips working together with the POC detection system in Fig. 1g. The microfluidic chips mass fabricated by PMMA polymer with chambers of one, four, and nine are developed. The multiple chambers in the microfluidic chip can either be used for multiplexed biomarker detection or for the accurate characterization of the biomarker by diluting the biosample in different ratios. Figure 1g shows two kinds of portable POC instruments developed; one is in handheld size using a mobile phone camera to detect the fluorescence for low sensitivity biomarker detection and the other is in desktop size using a high-resolution microscopic camera for the high sensitivity POC detections, and both kinds can automatically draw the biosample into the microfluidics for detection and can report the data of the results through the software in a laptop computer.

Overall, the LSPR POC system we studied has the advantages of simple detection system, high sensitivity, high selectivity, mass productive, low cost, and multiplexed array detection.

Technology Development

Design of the Gold Nanostructures

As shown in Fig. 1 in the principle, we excite the fluorescence dyes with the plasmons generated by shedding light from the glass side of the gold nanohole array. Gold is selected for the LSPR chips because gold is a durable material with high stability for long-term storage of the chips after fabrication. Gold possess an prominent plasmonic peak around the wavelength of 600–700 nm at the water–gold interface where the "capturing antibody-antigen-detection antibody conjugated with fluorescence dyes" bioassay locates, thus red fluorescence dye Alexa 647 is used in our experiments. The gold nanohole array provides much better plasmonic field for dye excitation than the randomly distributed gold nanoholes or islands/particles because it has narrower plasmonic wavelength band that can efficiently concentrate the optical power in a narrow wavelength band for fluorescence dye excitation. When the light incidence is from the glass side, the gold nanohole array blocks most of the transmission light and reduces the background noise for the dye emission detection. Furthermore, antifouling polymer layer can be synthesized in the gold nanohole array to raise the position of the fluorescence labels close to the places such as the top rims of the gold nanoholes where the plasmonic field is the strongest [17].

The commercially available COMSOL software (finite element method) for multiphysics analyses was employed to design the pitch, dimension, and the thickness of the gold nanohole array for exciting the fluorescence dye Alexa 647 [13–17]. Our simulation results found that the pitch is the most sensitive parameter in tuning the plasmonic peaks, the ratio of the LSPR wavelength tuning to the variation of pitch, hole diameter, and thickness are 1.1, 0.2, and 0.54, respectively. The gold nanohole array with pitch=400 nm, hole diameter=150 nm, and thickness=100 nm renders the highest field

intensity around the wavelength of 647 nm on the top rim of the gold nanoholes, and is thus used in our POC system.

The absorption (represents the plasmonic field and the heat dissipation on the gold), reflection, and transmission spectra of the gold nanohole array are plotted in Fig. 2. It has three plasmonic peaks in the absorption spectrum. The field distribution indicates that the first peak α at the wavelength of around 560 nm and the third peak γ at the wavelength of around 720 nm are LSPR modes at the gold–glass interface, while the β mode at the wavelength of 647 nm is at the gold–water interface that can be utilized for the enhancement of the fluorescence dyes.

Mass Fabrication of Gold Nanohole Array

The gold nanohole array for the LSPR POC system is mass fabricated in 4″ wafer level through nanoimprinting, with process drawn in Fig. 3a, which includes the fabrication of the nickel mold through e-beam writing and electroplating, and the nanoimprinting of the nanopatterns on the nickel mold onto a glass surface followed by photoresist residue removal and the gold film deposition and lift-off. After cleaning, the wafer is diced into small LSPR chips [13].

The scanning electron microscope (SEM) image of the fabricated gold nanohole array with the above designed size is presented in Fig. 3b. The only difference between the designed and the fabricated gold nanohole patterns is that the designed gold nanoholes are with diameter of 150 nm, while the e-beam written patterns are 140 nm long nanosquares, because we expect the gold nanoholes to be enlarged and will be degraded to a round shape after several fabrication steps. However, the nanosquares keep the square shape and the 140 nm size after the fabrication as shown in Fig. 3b, this is because our fabrication process is well optimized. The uniqueness of our fabrication includes the mold's nickel plating being directly conducted right after the e-beam resist development (without etching the silicon wafer), and the nanoimprinting is with UV curing photoresist which is with low nanoimprinting temperature and low pressure. They help on keeping the fidelity and high yield of our fabrication process.

The yield of our gold nanohole array fabricated on glass wafer is close to 100 % from nanoimprinting to gold lift-off, while the nickel mold has >70 % totally defect-free area. Compared with e-beam lithography, our technology can save the fabrication cost 50 or 100 times if the nickel mold can be used for 100 or 1,000 cycles. It is reported that a nickel mold is endurable with unnoticeable damage for thermal nanoimprinting up to 10,000 cycles [20], while our UV nanoimprinting can protect the mold better due to the low temperature and low pressure in process.

Capturing Antibody Orientation Control

It has been reported that the end-on orientation of the antibody where its constant fragment (Fc) is aligned upright and allows the active antigen binding fragment (Fab) to face the solution can improve the surface density of antigen binding sites up to 90 % and reduce the denature rate of the immobilized antibody [21, 22]. It is a surface modification technology that can be easily adopted in our LSPR chips.

Our surface immobilization technology is investigated using dual polarization interferometry (DPI), as illustrated in Fig. 4a, which is based on the interference of the light in a sensing and a reference waveguides for real-time extrapolation of the biomolecular interactions on the DPI chip's glass surface. Since it provides the interference of both TE and TM modes, the thickness, mass, density, and reflective index of the biomolecule are obtained simultaneously.

Exemplified by anti-PSA capturing antibody for PSA detection, we have investigated three orientation-controlled cAb immobilization methods: (1) protein G is used to grab the Fc region of IgG to make it upward [23]; (2) a boronic acid functionalized DPI chip is used to obtain the end-on orientation via chelation with the sugar resides (Fc); and (3) tris(2-carboxyethyl)phosphine (TCEP) reduction of the antibody creates antibody fragments that can lay on the surface via thiol-maleimide coupling, with the chemical immobilization processes illustrated in Fig. 4a.

In Fig. 4a, the anti-PSA cAb layer thicknesses for these methods are 8.8, 8.4, and 5.9 nm, respectively, while the randomly orientated cAb only exhibits a thickness of 3.3 nm [23], which clearly indicates the successful end-on

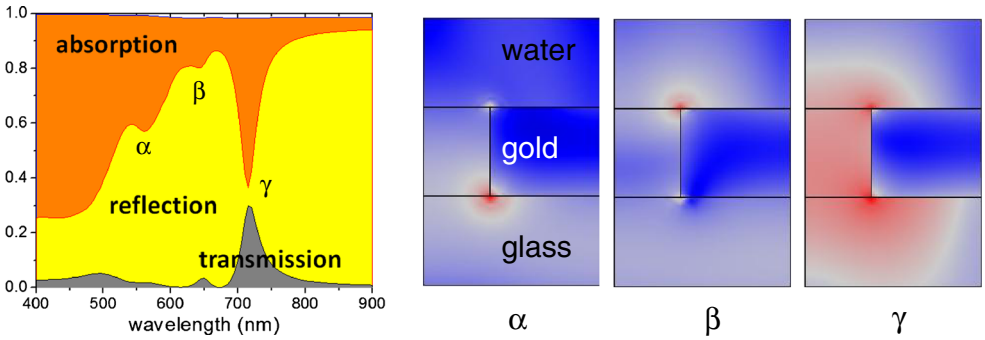

Fig. 2 The absorption, reflection, and transmission spectra of the gold nanohole array with the pitch of 400 nm, diameter of 150 nm, and thickness of 100 nm, with light incidence from the glass side. The nanohole array has three plasmonic peaks

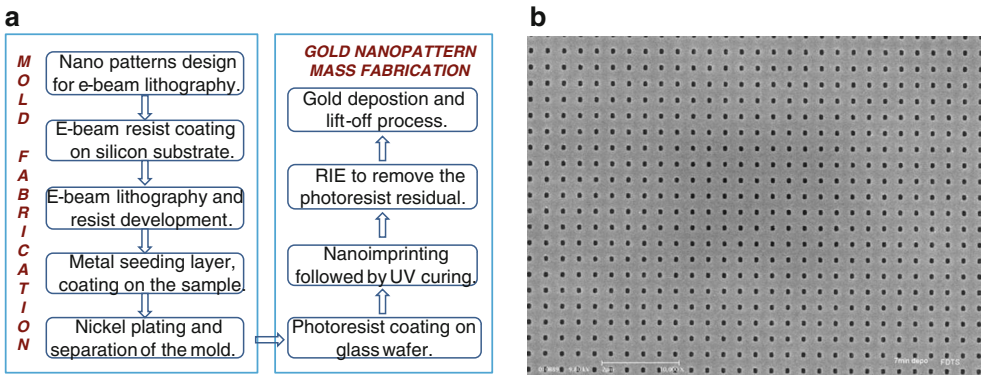

Fig. 3 Mass fabrication of gold nanohole array on 4″ glass wafter. **a** The fabrication process; **b** SEM image of the fabricated gold nanohole array on glass

immobilization in our methods. Among these three end-on immobilization methods, the affinity of the cAb with Protein G in method 1 is not very stable, while the chelation between boronic acid and sugar side chain in method 2 is sensitive to pH change in the buffer. Thus, method 3, TCEP cleft antibody immobilization, proves to be the most stable layer on the sensor chip due to the covalent coupling between the surface maleimide and cleft anti-PSA natural thiol. Figure 4b shows the sensitivity of method 3 is also about 100 times better than method 2. Because method 3 has the thinnest layer of the reductive antibody fragment, it would be beneficial for developing immunobiosensors using LSPR where the penetration depth of the plasmonic field into the buffer is only 15–30 nm.

We have also successfully immobilized the end-on cAb on gold substrate for SPR detection. Figure 4c shows when using SPR to detect PSA through a sandwich bioassay of "cAb-PSA-detection antibody", the orientation controlled by protein G can detect PSA of 1 pg/ml (as drawn in Fig. 1c), while randomly orientation cAb only can detect 1 ng/ml of PSA, the difference is 3 orders. This also means that for LSPR chips, we can selectively bind the cAb on gold or glass surface based on our plasmonic structure design.

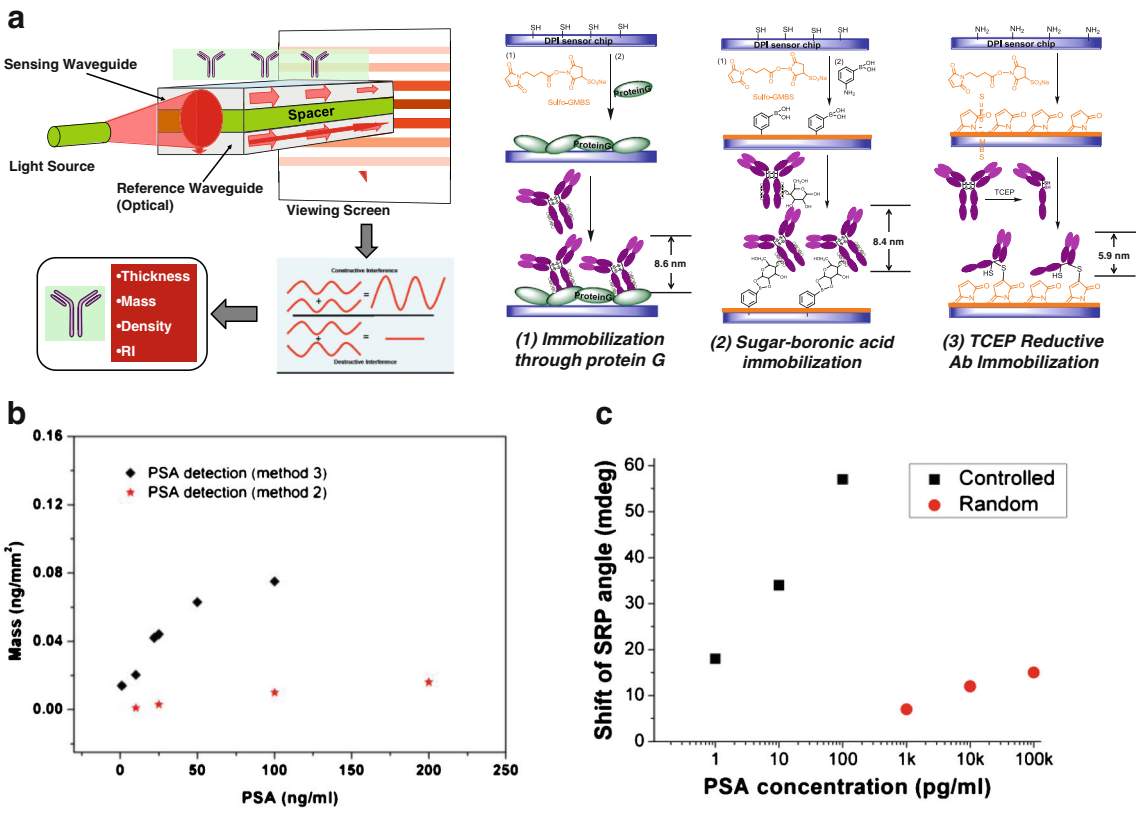

Fig. 4 The end-on immobilization of anti-PSA cAb. **a** The DPI principle and end-on immobilization processes for different end-on methods on the glass substrate of DPI. **b** The sensitivity comparison of the sugar boronic acid and TCEP methods, which present the sensitivity of 10 ng/ml and 100 pg/ml, respectively, by directly applying PSA on the cAb layer. **c** SPR detection for the protein G controlled and randomly orientated cAb for PSA detection through a sandwich assay of "cAb-PSA-detection antibody"

Antifouling Polymer

Antifouling POEGMA polymer can block the binding of proteins on its surface unless the ones with special links [24, 25], thus its properties are heavily investigated by us. It is verified that POEGMA can be selectively synthesized on gold or glass surface (Fig. 5a), can withstand most of the microfluidic fabrication process except plasma, and the polymer thickness can be varied by synthesis time (Fig. 5b). As the polymer thickness increases, its nonfouling effect enhances (Fig. 1d).

In more detail, Fig. 5a demonstrates that in the bright field image, the SiO2 patterns can be seen on the substrate no matter the POEGMA exists on the SiO2 surface or not. But in the dark-field fluorescence detections, false binding causes some fluorescence dyes to attach on the SiO2 without POEGMA; while POEGMA polymer on SiO2 totally eliminates the false binding and renders a totally dark fluorescence image.

The critical size of the pattern with POEGMA in Fig. 5a is about 20 μm. It is very challenging to synthesize the POEGMA directly inside the glass substrate of the gold nanoholes as we planned, and we are the first group working on it. Thus, in this paper, we initiate the glass surface with aminopropyl triethoxysilane (APTS), and use hexanedithiol (HDT) self-assembled monolayer acting as a passivating layer on gold to prevent nonspecific growth of POEGMA. The AFM images of the fabricated gold nanoholes before and after MUA/POEGMA growth are shown in Fig. 5c, and the success rate is around 37 %; about 37 % of the nanoholes are with POEGMA synthesized. Although the technology of synthesizing POEGMA directly inside the nanoholes is not ready for application yet, it demonstrates high potential of being used in our LSPR POC system in the near future.

Microfluidics with Multiple Chambers

We have designed and fabricated the microfluidics for LSPR POC system with up to nine chambers. The principles for the one, four, or nine chambers are the same, and the more chambers included, the more complicated the POC system will be in order to handle the sample dilution in each chamber.

The nine-chamber microfluidic chip is in credit card size and designed for antibody–antigen conjugation immunosensing with LSPR enhanced fluorescence emission, and it will be inserted into the LSPR POC instrument for optical-based imaging sensing, where excitation light emits from the bottom of the chip and the emission of the dyes are detected from the top.

The nine-chamber microfluidic chip has four layers, as illustrated in Fig. 6a–c. Layer 1 consists of microchannels for mixing, layer 2 is with wide channels for optical detection, layer 3 is for holding the LSPR glass chip (yellow chip in Fig. 6c), and layer 4 storages the waste liquid. The layer 1 can also be formed by two sublayers including a cover and a layer with open-through channels for the fluidics. The nine-channel microfluidic chip is fabricated by laser cutting and bonding the PMMA layers altogether at a temperature lower than 100 °C, thus it is inexpensive and disposable.

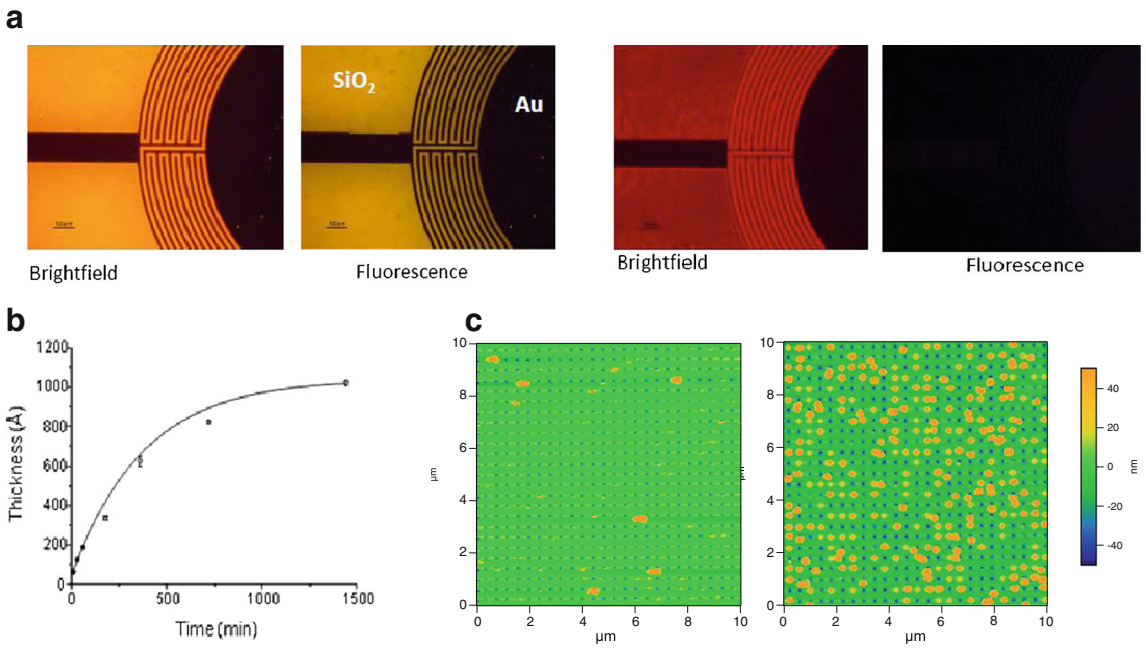

Fig. 5 **a** The selective nonfouling effect of POEGMA on different materials. SiO2 is patterned on a gold film. In the *left* two images, no POEGMA exists, while on the *right* two images, POEGMA is selectively synthesized on SiO2. **b** Ellipsometric thickness of polymer brush as a function of time. **c** Based on our POEGMA synthesis method, 37 % of the 140-nm-sized gold nanoholes are with POEGMA filled inside

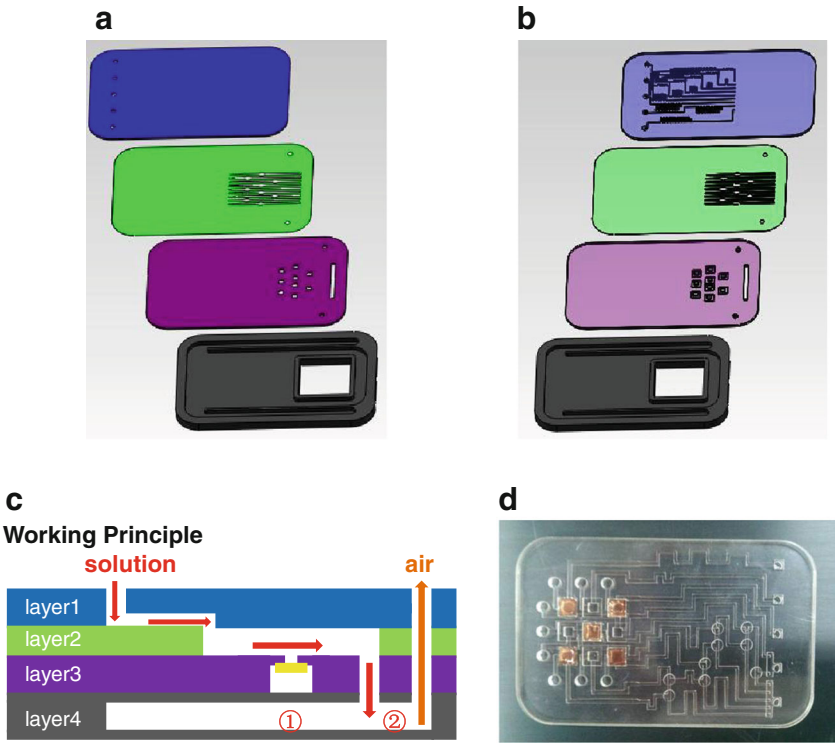

Fig. 6 The nine-chamber microfluidic chip. **a** The front view, **b** the back view, **c** the working principle, and **d** the fabricated chip

POC Prototype Fabrication

Two versions of the POC systems are fabricated. The first version is with mobile phone as shown in Fig. 7a, b. It proves that POC system can be compact enough using a smartphone and off-the-shelf electronic components, but power consumption is a major issue especially for spectroscopic measurement. The LSPR signal intensity is too low to be feasible with this handheld design, because the smartphone camera using CMOS imaging IC does not have low background noise required by LSPR detection nor does it have enough dynamic range for the low level LSPR signal (gain of

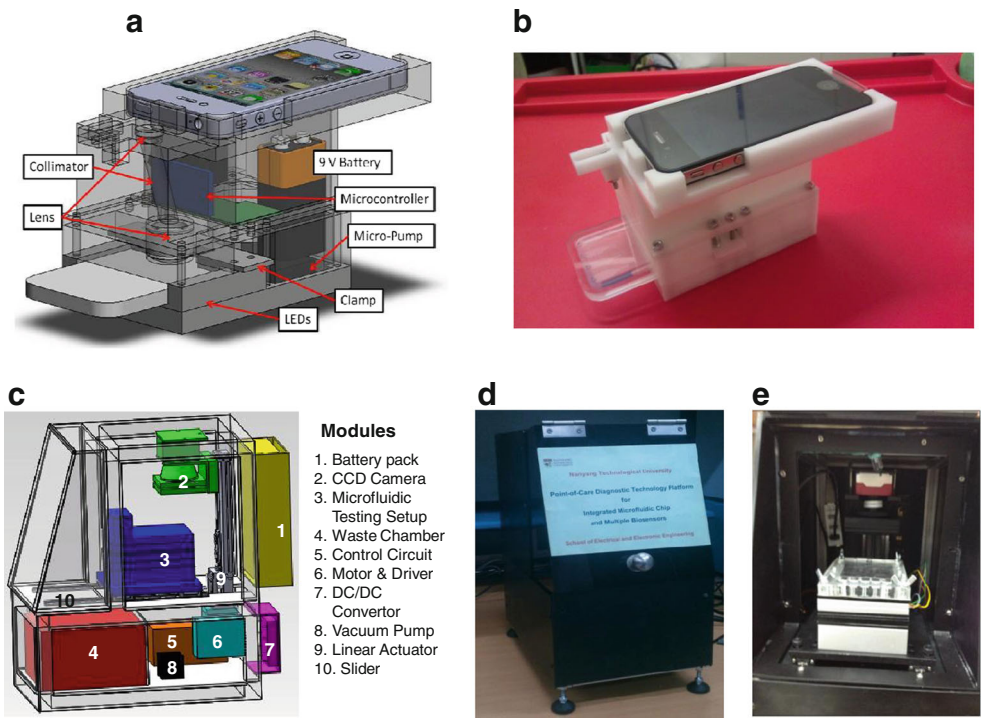

Fig. 7 The design and fabricated POC prototypes for the LSPR biosensing. **a** The principle and **b** the fabricated handheld POC based on mobile phone camera, **c** the principle, and **d**, **e** the fabricated desktop POC based on microscope camera

100 to 1,000 only). However, the handheld POC is still applicable for other biosensing diagnostic methods with stronger detection signal.

Thus for the second version, a desktop POC system was developed. It costs about 5,000 SGD, but the price can be reduced to 2,000~3,000 SGD upon further simplification. To save the effort, the design of low power electronic circuitry for both POC and desktop system is common. The design of the system is shown in Fig. 7c, and the fabricated POC system is photographed in Fig. 7d, e. Its overall size is 200 mm (width)×300 mm (depth)×350 mm (height), the power supply is a battery pack with AC charger, and the material of construction is black anodized aluminum.

The POC design has no lens, and the position of the camera will be automatically adjusted for focusing by controlling software and the mechanical system. Upon operation, because the testing setup and microfluidic chip are connected to waste chamber, vacuum is turned on in waste chamber for suction of fluidics, with microfluidic flow of the analyte, diluent, calibration, and reference samples controlled by software. As the bioassay is established in the POC system and ready for detection, LED lamp on the bottom of the chips excites the fluorescence dyes. The dyes in dark-field will generate an optical image taken by top camera after passing through interchangeable built-in optical filters to select only the emission from the fluorescence tags, and the microscope camera provides enhanced detection sensitivity suitable for weak LSPR signal detection. The operation of the fully integrated POC system is user-friendly by just inserting the microfluidic chip and pressing a button.

Characterization of the Integrated Subsystems

The LSPR Chips for Biosensing

In order to verify the effectiveness of the LSPR chip design and quality of the chip fabrication, PSA was detected through a (c-Ab)-antigen-(d-Ab) sandwich immunoassay by using a home-made total internal reflection (TIR) fluorescence spectroscopy under the TE mode. In the TIR fluorescence system, the light at the wavelength of 633 nm was shed from the bottom of a prism at a total reflection angle of 71°. Under the TE mode, no surface plasmon resonance generated on the gold film or the gold nanohole array. The LSPR on the gold nanohole array is polarization independent, thus the dye excitations are enhanced by the LSPR [13].

The results in Fig. 8a show that fluorescence intensity presents a linear increment of 500 times, when the PSA concentration was increased from 100 pg/ml to 100 ng/ml. The limit of detection (LOD) was determined to be 100 pg/ml, based on three times of the standard deviation of the fluorescence response for blank samples. In the control experiment, the gold film only achieved a LOD of 1,000 pg/ml. This LOD difference is because under the TE mode, there is no plasmonics generated on the gold film, while the gold nanohole array still generates LSPR to enhance the fluorescence excitation.

To further investigate the plasmonic field distribution difference of the gold nanohole array and the gold film, simulation results of the transmission spectra are shown in Fig. 8b, c. It confirms that there is a LSPR field distributed at the top rims of the gold nanoholes, while there is no obvious field intensity on the gold film surface. However, based on the transmission spectrum in Fig. 8b, 10 % of the light is transmitted to the top of the gold film surface, where the dyes are bound in the control experiment. So the dyes are still excited in the TE mode for the gold film, although the excitation is weak compared to the gold nanohole array.

The Dilution in Microfluidics with Desktop POC

The nine-chamber can be used with six for analyte sample, two for standard references, and one for system calibration; or six channels for reference/calibrations, two for analyte, and

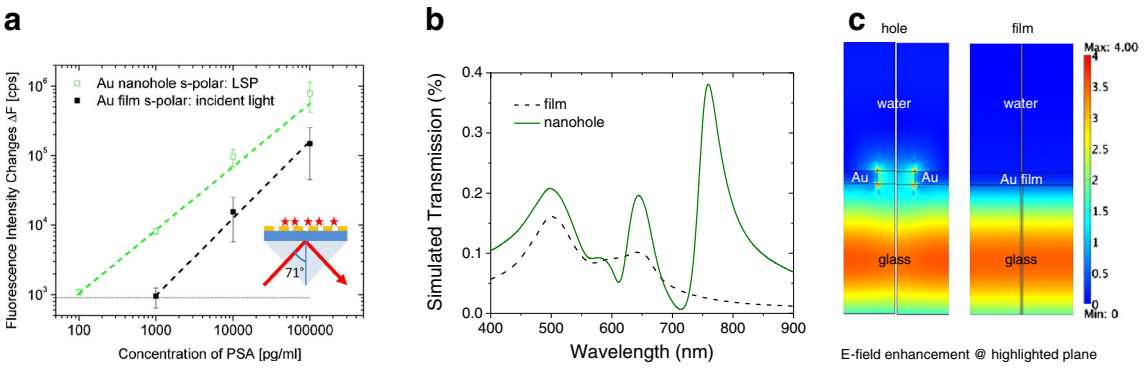

Fig. 8 **a** Fluorescence detections on gold nanohole array (pitch=400 nm, square length=140 nm, thickness=50 nm) and gold film (thickness=50 nm) for the sandwich immunoassay of PSA at the concentrations from 100 pg/ml to 100 ng/ml, when the 633 nm light sheds at 71° to the TIR fluorescence spectroscopy in TE mode. **b** The transmission spectra and **c** the plasmonic field distributions of the gold nanohole array and gold film on glass under the same conditions as in the experiments

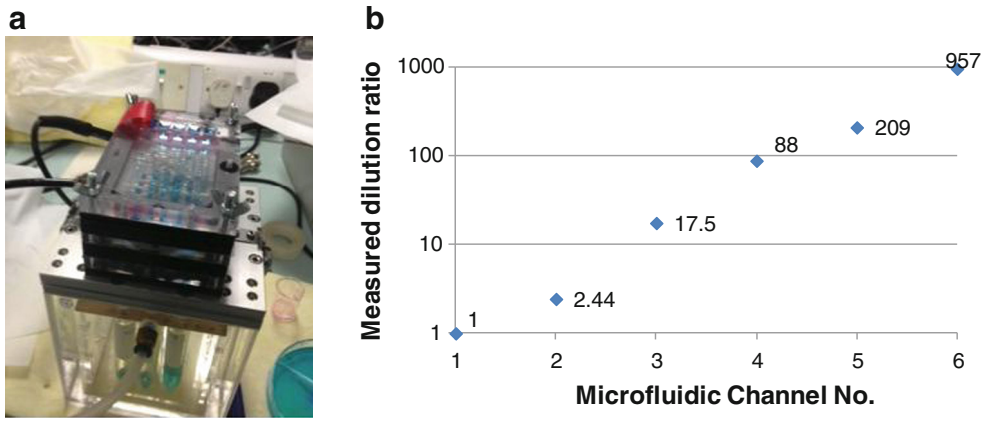

Fig. 9 **a** Dilution and flow-rate test jig setup for microfluidic chip detection and **b** the measured sample dilution ratios in six channels

one for system calibration. In any case, six chambers will have buffers with different dilution ratios.

A dilution and flow-rate test jig was fabricated as shown in Fig. 9a. In Fig. 9a, sample fluid flowing out of the microfluidic channels is collected by nine plastic test tubes (put inside the waste chamber setup), and the target performance is to achieve the dilution in different channels. Figure 9b demonstrates that the nine chambers are satisfactory diluted in a linear response in logarithmic scale, which is required in biosensing characterizations.

The Image Qualities of Desktop POC

Some test results, including the images of front side illumination of bright field with and without filters, and dark-field noise, are presented in Fig. 10. These images are in high resolution that satisfied the fluorescence dye detections as in a dark-field microscope system.

The tests showed that if the images are taken by long exposure time (5.5 s), the noise detected by the camera will be saturated and cannot be averaged out. If the exposure time is short (0.3 s), the noise will be eliminated by averaging based on Gaussian mixture distribution model (GMM). Thus, in order to remove pixel saturation and noise, the image will be taken at 0.3 s exposure for the noise environment to be modeled. The summation of processed images can be effectively used at any exposure more than 10 s.

Conclusion

This paper introduced the key technologies in developing a LSPR-based POC system. Since POC systems tend to have lower sensitivity due to the smaller size and cheaper components, we used LSPR to enhance the excitation of the fluorescence labels so as to increase the sensitivity of the LSPR POC system for medical diagnostics. The LSPR caused sensitivity enhancement is 10 higher than that of a gold film for PSA biomarker detection. Besides, another two strategies on bioassay's surface modification including the antibody orientation control and antifouling POEGMA were investigated, which can be readily translated into the LSPR chips. The disposable plastic microfluidic chips with one, four, or nine chambers are designed and fabricated. For the nine-chamber microfluidic chip, six channels can be diluted in logarithmic ratio of up to 1,000 times for the characterization of the analyte. The microfluidic chip can be easily inserted into our fabricated desktop POC system, and automatic detection of the chip has been realized by software, including the system initiation, sample dilution, and image analyses. The next step of our work will be the integration of the capturing antibody orientation control and antifouling POEGMA into the LSPR bioassays on the LSPR chip, and the use of the fabricated nine-chamber microfluidic chip and the LSPR POC system for PSA detection. Overall, our work provides a good example on how to select and combine different technologies to

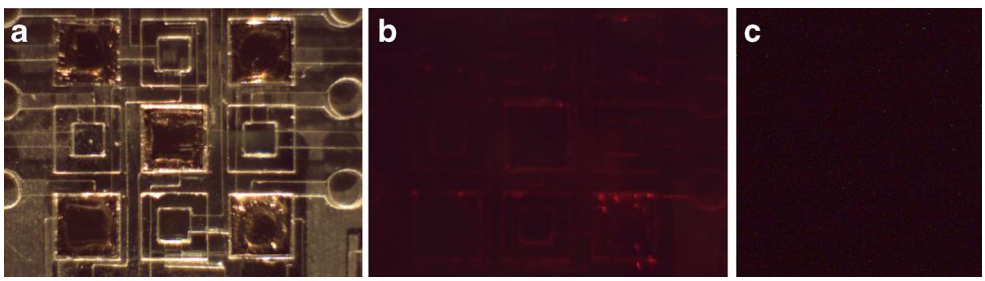

Fig. 10 The images taken by the camera inside the POC system, with **a** gold film without nanoholes lighted from top. **b** Images of the chip with white LED light passing through a 590 nm long-pass filter. **c** Image taken at 5.5-s exposure. As evident from image, there are some pixel saturation and electrical noise

miniaturize a bulky biosensing instrument into a user-friendly POC system, while offering the potential of high performance.

Acknowledgments We acknowledge SERC, A*STAR for its financial support of the project 102 152 0014. The LSPR chips were fabricated and characterized the SERC nanofabrication, processing, and characterisation (SnFPC) at the Institute of Materials Research and Engineering (IMRE); the authors are indebted to the kind help from the SnFPC staffs.

References

1. Liedberg B, Nylander C, Lundström I (1983) Surface plasmon resonance for gas detection and biosensing. Sensors Actuators 4:299–304
2. Homola J (2003) Present and future of surface plasmon resonance biosensors. Anal Bioanal Chem 377(3):528–539
3. Homola J, Yee SS, Gauglitz G (1999) Surface plasmon resonance sensors: review. Sensors Actuators B Chem 54:3–15
4. Haes J, Stuart DA, Nie S, Van Duyne RP (2004) Using solution-phase nanoparticles, surface-confined nanoparticle arrays and single nanoparticles as biological sensing platforms. J Fluoresc 14(4):355–367
5. Willets KA, Van Duyne RP (2007) Localized surface plasmon resonance spectroscopy and sensing. Annu Rev Phys Chem 58:267–297
6. Zhao J, Zhang X, Yonzon C, Haes AJ, Van Duyne RP (2006) Localized surface plasmon resonance biosensors. Nanomedicine 1:219–228
7. Zhou X, Knoll W, Liu KY, Tse MS, Oh S, Zhang N (2008) Design and fabrication of gold nanostructures with dispersed nanospheres for localized surface plasmon resonance applications. J Nanophotonics 2:023502
8. Sannomiya T, Scholder O, Jefimovs K, Hafner C, Dahlin AB (2011) Investigation of plasmon resonances in metal films with nanohole arrays for biosensing applications. Small 7(12):1653–1663
9. Yu F, Yao DF, Knoll W (2003) Surface plasmon field-enhanced fluorescence spectroscopy studies of the interaction between an antibody and its surface-coupled antigen. Anal Chem 75:2610–2617
10. Yu F, Persson B, Lofås S, Knoll W (2004) Surface plasmon fluorescence immunoassay of free prostate-specific antigen in human plasma at the femtomolar level. Anal Chem 76:6765–6770
11. Yu F, Persson B, Lofås S, Knoll W (2004) Attomolar sensitivity in bioassays based on surface plasmon fluorescence spectroscopy. J Am Chem Soc 126:8902–8903
12. Besselink GAJ, Kooyman RPH, van Os PJHJ, Engbers GHM, Schasfoort RBM (2004) Signal amplification on planar and gel-type sensor surfaces in surface plasmon resonance-based detection of prostate-specific antigen. Anal Biochem 333:165–173
13. Wong TI, Han S, Wu L, Wang Y, Deng J, Tan CYL, Bai P, Loke YC, Yang XD, Tse MS, Ng SH, Zhou X (2013) High throughput and high yield nanofabrication of precisely designed gold nanohole arrays for fluorescence enhanced detection of biomarkers. Lab Chip 13:2405–2413
14. Wang Y, Wu L, Zhou X, Wong TI, Zhang J, Bai P, Li EP, Liedberg B (2013) Incident-angle dependence of fluorescence enhancement and biomarker immunoassay on gold nanohole array. Sensors Actuators B Chem 186:205–211
15. Wu L, Bai P, Zhou X, Li EP (2012) Reflection and transmission modes in nanohole-array-based plasmonic sensors. IEEE Photon J 4:26–33
16. Wu L, Bai P, Li EP (2012) Designing surface plasmon resonance of subwavelength hole arrays by studying absorption. J Opt Soc Am B 29:521–528
17. Bai P, Zhou X, Wu L (2013) Sensor and method of detecting a target analyte. US 20130112857 A1
18. Tabakman SM, Lau L, Robinson JT, Price J, Sherlock SP, Wang H, Zhang B, Chen Z, Tangsombatvisit S, Jarrell JA, Utz PJ, Dai H (2011) Plasmonic substrates for multiplexed protein microarrays with femtomolar sensitivity and broad dynamic range. Nat Commun 2(466):1–9
19. Rivoire K, Kinkhabwala A, Hatami F, Masselink WT, Avlasevich Y, Müllen K, Moerner WE, Vučković J (2009) Lithographic positioning of fluorescence molecules on high-Q photonic crystal cavities. Appl Phys Lett 95(12):123113 1–3
20. Rai-Choudhury P (ed) (1997) Handbook of microlithography, micromachining and microfabrication. Volume 2: Micromachining and Microfabrication (SPIE PRESS Monograph Vol. PM40). Society of Photo Optical, p 349
21. Trilling AK, Beekwilder J, Zuilhof H (2013) Antibody orientation on biosensor surfaces: a minireview. Analyst 138(6):1619–1627
22. Cho I-H, Paek E-H, Lee H, Kang JY, Kim TS, Paek S-H (2007) Site-directed biotinylation of antibodies for controlled immobilization on solid surfaces. Anal Biochem 365:14–23
23. Song HY, Zhou X, Hobley J, Su XD (2012) Comparative study of random and oriented antibody immobilization as measured by dual polarization interferometry and surface plasmon resonance spectroscopy. Langmuir 28(1):997–1004
24. Hucknall A, Kim D-H, Rangarajan S, Hill RT, Reichert WM, Chilkoti A (2009) Simple fabrication of antibody microarrays on nonfouling polymer brushes with femtomolar sensitivity for protein analytes in serum and blood. Adv Mater 21:1968–1971
25. Ferhan AR, Guo LH, Zhou X, Chen P, Hong SP, Kim D-H (2013) Solid-phase colorimetric sensor based on gold nanoparticle-loaded polymer brushes: lead detection as a case study. Anal Chem 85(8):4094–4099